Symposium: Chemistry at the Nanometer Scale

edited by
K. W. Hipps
Washington State University
Pullman, WA 99163

Electrochemical Fabrication of Metallic Quantum Wires

Nongjian Tao
Department of Electrical Engineering & Center for Solid State Electronics Research, Arizona State University, Tempe, AZ 85287; *nongjian.tao@asu.edu*

The recent surge of interest in nanostructured materials and devices is often attributed to the ever-increasing need of miniaturization and integration of electronic devices. An equally important reason for studying nanostructured materials and devices is that they often exhibit novel properties that may revolutionize technologies, from chemical and biological sensors to electronic, optical, and mechanical devices. Some of the novel properties arise from various quantum effects that become pronounced as materials and devices are reduced to the nanometer scale. Although some quantum effects can be observed only in ultrahigh vacuum at cryogenic temperatures, others are robust and can be studied even in "dirty" environments, such as in air, in solvents, and in electrolytes at room temperature. The nanostructures that exhibit the quantum effects can be easily fabricated with inexpensive setups. The purpose of this article is to discuss one such nanostructure, metallic quantum wires.

In this article we introduce some basic quantum transport concepts to readers who have no prior knowledge on the subject. We next focus on how to fabricate metallic quantum wires using simple electrochemical techniques. Finally we discuss some possible applications and provide a summary.

Quantum Phenomena in Nanostructures

A basic quantity that describes how electrons (or charged carriers) move through a material or device is resistance (R), which is defined as the ratio of the voltage applied across the material to the consequent current in the material. For a wire-like sample, classical physics says that the resistance is given by

$$R = \rho\frac{L}{A} \qquad (1)$$

where ρ is the resistivity of the material and L and A are the length and the cross-sectional area of the wire, respectively. The inverse of R in eq 1 is defined as conductance, G. The resistivity of such a classical wire is a physical property that depends on the material of the wire, but it does not generally depend on the length or diameter of the wire. However, when the sample dimensions are decreased below certain characteristic lengths, quantum effects make ρ depend on the sample dimensions. In this section we discuss why the well-known classical relation given by eq 1 breaks down and what new phenomena arise when the sample is reduced to the nanometer scale. We provide a brief description of Landauer's view of resistance (or conductance), introduce the concept of characteristic lengths, and then discuss how the size of a material can drastically change the electron-transport properties of the material.

Landauer Formula

Electric current has often been viewed as the response of charges in a material to an applied electric field or voltage. In contrast, Landauer viewed current as a transmission process, or a consequence of the injection of electrons at one end of a sample and the probability of the electrons to reach the other end. This view has proven to be extremely useful to understand electron-transport processes in nanostructured materials and devices, including molecular systems *(1, 2)*.

Landauer's original result was obtained for a system of two leads connecting to a sample. The two leads in the system are connected to two macroscopic electrodes (also called electron reservoirs) (Figure 1). The sample is where scattering of electrons can take place, which is characterized by the

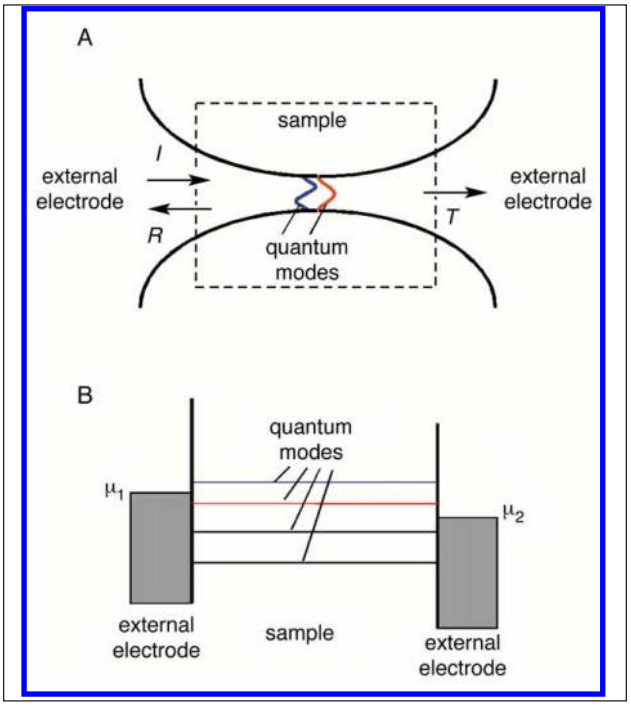

Figure 1. (A) A quantum wire (sample) is connected to two electrodes. The curved lines represent a smooth transition between the leads and the sample (in dashed box). In the transverse direction, electrons form quantum modes (standing waves). I, R, and T represent incident, reflected, and transmitted electron waves, respectively. (B) Energy diagram of the system, where μ_1 and μ_2 (Fermi energy levels) are the chemical potentials of the two electrodes, and the horizontal lines are the energy levels of the quantum modes. The difference, $\mu_1 - \mu_2$, is maintained by an external voltage source. The lines represent the energy levels of the quantum modes formed in the transverse direction.

transmission-probability function, $T(E)$. The conductance (G) of the system at a small applied bias voltage (V) is given by

$$G = \frac{I}{V} = \frac{2e^2}{h}T(E_F) \quad (2)$$

where e is the electron charge and h is the Planck constant. $T(E)$ is a dimensionless quantity, and the prefactor, $2e^2/h = 77.4\ \mu S$, is called the conductance quantum. The inverse of the conductance quantum is $h/(2e^2) = 12.9\ k\Omega$, called the resistance quantum.

Equation 2 is for a one-dimensional wire sample in which only one quantum mode exists in the direction normal to the propagation direction or only one channel for the conduction electrons to access, like traffic on a one-lane highway. If the sample has a finite width, electrons in the normal direction form a series of quantum modes like standing waves in a violin string or particles in a potential well (Figure 1). The de Broglie wavelength of the conduction electrons is λ_F, which is given by $\lambda_F = 2\pi/(2mE_F)^{1/2}$, where E_F, the energy of the conduction electrons (at moderate temperature and bias voltages), is called the Fermi energy (chemical potential). For a two-dimensional wire of width W, the number of quantum modes or standing waves, N, is simply determined by the ratio of the width of the wire to λ_F. For example, if $W < (\lambda_F/2)$, no standing waves can exist and $N = 0$. If $\lambda_F > W > (\lambda_F/2)$, one standing wave is formed since the condition for the first standing wave is $W = (\lambda_F/2)$, and $N = 1$. So in general, $N = \mathrm{INT}(2W/\lambda_F)$, for a two-dimensional wire. For a three-dimensional cylindrical wire, a wave equation needs to be solved to determine N, but it also increases in discrete steps with the wire width *(3)*. In this multiple-mode case, the Landauer formula can be generalized to the form of

$$G = \frac{2e^2}{h}\sum_{i,j}^{N} T_{ij}(E_F) \quad (3)$$

where T_{ij} is the probability that an electron transmits from the ith mode at the left of the sample to the jth mode at the right of the sample. The summation is over all the quantum modes with nonzero T_{ij} values. For an ideal transmission, T_{ij} is 1 for $i = j$ and 0 for all other cases, and eq 3 is simplified as $G = NG_0$, where $G_0 = 2e^2/h$. Since N is always an integer that increases with the wire width, the conductance increases in a stepwise fashion with the wire width, which is sharp contrast to the classical wires. This phenomenon is conductance quantization and the wire is sometimes referred to as quantum wire, or quantum point contact.

It is rather straightforward to see how the Landauer formula leads to conductance quantization, but we have not yet answered the question under what conditions one expects to observe the phenomenon. This is the next subject of discussion.

Characteristic Lengths

We have stated that new quantum phenomena occur when the sample is small enough. In order to determine how small is small enough, we need some characteristic lengths to describe the system. The following three characteristic lengths are useful for in understanding the transition from classical to quantum regimes. The first one is the Fermi wavelength, λ_F, which was introduced earlier. The second is the momentum-relaxation length, L_m, which describes the average distance an electron can travel before colliding with impurities or defects in the sample *(4)*. This is often referred to as the electron mean free path. The third useful characteristic length is the phase-relaxation length (or coherence length), L_ϕ, which is the length over which an electron retains its coherence as a wave *(2)*. If a sample is smaller than L_ϕ, the electron waves can interfere with each other.

L_m and L_ϕ are determined by the scattering of a propagating electron wave by defects, impurities, phonons (vibrations of atoms), and other electrons. For an elastic scattering in which the electron does not lose or gain energy, the electron will change its momentum but not its wave coherence. This is like the reflection of a light wave by a mirror that changes the momentum (direction) but not coherence of the light wave. So elastic scattering contributes to L_m but not to L_ϕ. If the scattering results in a change in the electron energy (called inelastic scattering) that occurs when the propagating electron wave excite core electrons, phonons, and spins associated with magnetic impurities, the phase of the electron wave is lost in addition to a change in the electron momentum. Thus inelastic scattering contributes to both L_ϕ and L_m. Scattering events between two conduction electrons are more complicated. In general, they contribute to L_ϕ only, but not to L_m *(2)*.

The above characteristic lengths can be changed by varying experimental parameters or by changing the material properties. For example, by lowering the temperature the excitation of phonons can be suppressed, which can increase both L_m and L_ϕ. In elastic and magnetic scattering, the concentrations of ionic and magnetic impurities vary from sample to sample, which may also be controlled. Furthermore, the magnetic scattering can be suppressed by a magnetic field. The electron–electron interaction is determined by the carrier concentration and the energy band structure. So different transport properties and mechanisms can be studied by preparing materials and by controlling external experimental parameters.

Using the three characteristic lengths, we can divide electron transport into three regimes: ballistic, diffusive, and classical transports. Ballistic transport occurs with no significant momentum and phase relaxation. Diffusive transport involves many elastic-scattering events and thus losing momentum information, but the electrons remain coherent (no substantial phase relaxation). This situation arises because an elastic-scattering event can change the electron momentum but retain the wave coherence (like reflection or scattering of a light wave by an object). This is analogous to a coherent light wave (say laser beam) propagating in a medium containing many particles where the transmitted wave is determined by the interference of many scattered waves. Classical transport is the case where both electron momentum and phase relaxation occur frequently, so the wave interference during a series of scattering events can be neglected and an electron can be considered as a particle.

Ballistic Transport (Sample Length << L_m and L_ϕ)

This case is called ballistic transport because an electron wave can prorogate through the sample without experiencing scattering that can change its momentum or phase. The conductance in this case is quantized and given by $G = NG_0$,

according to the Landauer formula discussed above. One may wonder why the conductance is still finite even if the electrons transport ballistically through the sample. This can be understood by the following considerations. We start with the Landauer formula (eq 3),

$$G = NG_0T \tag{4}$$

where $T = \sum_j T_{ij}(E_F)$ is the transmission probability for electrons from a channel at the left side of the sample to the right side. The resistance of the system is

$$R = \frac{h}{2e^2}\frac{1}{NT} \tag{5}$$

which includes both the resistance of the sample, R_s, and the contact resistance, R_c, between the sample and the leads. When $T = 1$, we may note that the sample resistance is zero, which means that the resistance must be entirely due to the contacts, so

$$R_c = \frac{h}{2e^2}\frac{1}{N} \tag{6}$$

The resistance of the sample is then given by

$$R_s = R - R_c = \frac{h}{2e^2}\frac{1}{NT} - \frac{h}{2e^2}\frac{1}{N} = \frac{h}{2e^2N}\frac{1-T}{T} \tag{7}$$

Classical Transport (Sample Length >> L_m >> L_ϕ)

In this case, the electron waves traveling from the left side experience many scattering events before reaching the right side of the sample. We also note that the electron waves are no longer coherent throughout of the entire sample, so one cannot solve the Schrödinger equation over the entire sample. Furthermore, since $L_m >> L_\phi$, we can neglect the interference effect during a series of scattering events, which means that the total transmission probability is determined by the individual transmission and reflection events at the scattering centers. Let us consider two such scattering centers. The transmission probability after the first scattering center is T_1, and the transmitted wave will partially transmit through the second scattering center with a probability of T_1T_2 and be partially reflected by the second scattering center with a probability of T_1r_2, where r_2 is the reflection probability at scattering center 2. The reflected wave traveling in the backward direction will encounter the first scattering center and be reflected to the forward direction with a probability of $T_1r_2r_1$ (r_1 is the reflection probability at scattering center 1). This forward-going wave will again partially transmit through the second scattering center with a probability of $T_1r_2r_1T_2$ and be partially reflected by it with a probability of $T_1r_2r_1T_2r_2$. The reflected wave will go through similar transmission and reflection events. So the total transmission probability is given by

$$T_{12} = T_1T_2\left(1 + r_1r_2 + r_1^2r_2^2 + \ldots\right) = \frac{T_1T_2}{1 - r_1r_2} \tag{8}$$

where the series arises because the electron wave can reflect back and forth many times between the two scattering centers. After substituting $r_1 = 1 - T_1$ and $r_2 = 1 - T_2$ into eq 8, we can rewrite it into

$$\frac{1 - T_{12}}{T_{12}} = \frac{1 - T_1}{T_1} + \frac{1 - T_2}{T_2} \tag{9}$$

According to eq 7, we have

$$R_{10} = R_1 + R_2 \tag{10}$$

If we generalize the above results to N scattering events, the total resistance is the sum of N microscopic resistances, each determined by a scattering event. Assuming that the scattering centers are uniformly distributed along the wire, we can conclude that the total resistance is proportional to the wire length. This is the classical behavior described by eq 1.

Diffusive Transport (Sample Length> L_ϕ >> L_m)

We have assumed in the previous case (classical conductor) that the phase becomes random after a scattering event. When $L_\phi >> L_m$, the phase of the electron wave can shift by a certain quantity but is not completely lost (random). In this case, the resistance due to two scattering centers is given by

$$R_{12} = R_1 + R_2 + \Delta \tag{11}$$

where Δ is due to the interference between the waves scattered from the two scattering centers. It is clear that R_{12} is not a simple sum of R_1 and R_2, so the classical result given by eq 1 is not valid. It can be shown that the nonadditive term in eq 11 causes an exponential divergence for R as a function of L (sample length) *(2),*

$$R \sim e^{2L/L_m} - 1 \tag{12}$$

Resistance is very large for large L and the material becomes an insulator. This is known as the localization phenomenon.

Electrochemical Fabrication of Quantum Wires

To observe quantum effects, the dimensions of a nanostructure must be small in comparison to the characteristic length scales described above. The characteristic lengths depend on the intrinsic properties of the material, temperature, and other external parameters. Many quantum phenomena were initially observed and studied in semiconductor nanostructures because the characteristic lengths of the semiconducting materials can be rather large. For example, for the GaAlAs heterostructure in which the first conductance quantization was observed *(5, 6),* the Fermi wavelength is ~50 nm and the mean free path is several micrometers at low temperatures. Structures of these dimensions can be fabricated using electron beam lithography techniques. However, the relatively large Fermi wavelength means that the energy separation between quantum modes is small in comparison to room temperature thermal energy. This is why conductance quantization and other quantum phenomena in semiconducting nanostructures were often observable only at low temperatures. In the case of metallic materials, the wavelength and mean free path are much smaller. For example, the wavelength of a typical metal, such as Cu, is only a few hundred pm, the size of an atom, and the mean free path is a few tens of nm *(4).* The

small wavelength means that conductance quantization in metal wires is pronounced even at room temperature, but the diameter of the wires must be comparable to the size of an atom and the length must be shorter than a few tens of nm.

One can use two basic approaches to fabricate such nanowires. One is the mechanical method, which creates an atomic-scale wire by mechanically separating two electrodes in contact *(7–11).* During the separation process, a metal neck is formed between the electrodes owing to the strong cohesive energy of the metal, which is stretched into an atomically thin wire before breaking *(12).* The second method is based on electrochemical etching and deposition *(13–16)*, which is the main focus of this article.

Electrochemical Fabrication

Most electrochemical fabrication methods use either electrodeposition or etching of metals. In electrodeposition, a conductive object on which electrodeposition takes place serves as a cathode in an electrochemical cell *(17).* When the potential applied to the cathode is negative enough, metal ions in the electrolyte accept electrons from the cathode and are reduced on the cathode surface. The process can be regulated by controlling a number of parameters, including the potential or current, temperature and condition (roughness, clearness, etc.) of the cathode, and purity, concentration, and composition of the electrolyte. While aqueous electrolytes are commonly used, other metals, such as Ti and Al, can only be electrodeposited from organic electrolytes. Some metals, such as Mg, Nb, Ta, and W, can only be electrodeposited from molten salt electrolytes (at 700 °C and above). Electrochemical etching is a reverse process in which the conductive object is used as anode.

In contrast to vacuum-based techniques, electrochemical fabrication techniques are attractive not only because of their simplicity, but also because they have a number of unique features. Some of the features will be illustrated by examples described in the next section. To date, electrochemical techniques have been used to fabricate various nanostructures, from simple nanoclusters and nanowires to sophisticated mechanical devices. The methods used to fabricate the nanostructures can be divided into the following categories.

Local-Probe Method

This method *(18, 19)* uses a local probe, such as the tip of a scanning tunneling microscope (STM) or atomic force microscope (AFM), in close proximity to a metal or semiconductor surface to induce localized electrodeposition *(20–23),* etching *(24–29),* chemical reaction *(30),* or mechanical contact *(31, 32).* The method not only fabricates atomic-scale structures, but also allows one to visualize these structures. The local-probe method creates structures one at a time, so it is not (yet) suitable for mass-production of nanostructures.

Template Method

Nanostructures have been fabricated by confining electrodeposition and etching processes with various templates, including negative, positive, and surface-step templates. The negative-template method uses prefabricated cylindrical nanopores in a solid material as templates *(33–38).* By depositing metals into the nanopores, nanowires with a diameter predetermined by the diameter of the nanopores are fabricated. The positive template method uses wirelike nanostructures, such as DNA *(39, 40)* and carbon nanotubes *(41),* as templates to guide electrodeposition on the surface of the templates. Unlike negative templates, the diameters of the nanowires are not restricted by the template sizes and may be controlled by adjusting the quantity of material deposited on the templates. Atomic-scale step edges on crystal surfaces can be used as templates to grow nanowires *(42–44).* The process is based on the fact that electrodeposition often starts preferentially along surface step edges.

Property-Based Method

The local and the template methods described above control the shape and dimensions of a fabricated nanostructure, such as a nanowire. After fabrication, one then assembles the nanowire into an electrical circuit and measures the electron-transport properties of the nanowire. An opposite approach is to monitor the electron-transport properties constantly during the fabrication process *(13, 15, 29).* Once the properties become desirable, the fabrication process is stopped. So the measured electron-transport properties are used as a feedback signal to fabricate nanostructures with the desired properties. This is the method that has been used to fabricate metallic quantum wires, which is discussed in more detail below.

Fabrication of Quantum Wires

The first attempts to electrochemically fabricate metallic quantum wires used local probes, such as STM and AFM *(13, 15).* A simpler approach is to start with a metal wire supported on solid substrate (Figure 2) *(14).* The metal wire with an initial diameter of a few tens of μm is glued onto a glass slide. The glue covers the entire wire except for a small portion that is exposed to electrolyte for electrodeposition and etching. The exposed portion is less than a few μm so that ionic conduction through the electrolyte is negligible compared to the electronic conduction through the wire. By electrochemical etching, the diameter of the wire is reduced to the atomic scale on which the conductance becomes quantized. The process can be reversed to increase the diameter by electrodeposition. The etching and deposition are controlled with a bipotentiostat that can simultaneously control the etching rate and measure the conductance of the wire. The method has been used to fabricate atomic-scale Au, Ag, Cu, Zn, Pb, Pd, and Ni wires with quantized conductance *(45–47).*

More recently a simple self-limiting method has been demonstrated by Boussaad et al. *(48).* The method does not require a bipotentiostat and feedback control, and it can *simultaneously* fabricate an array of wires. It starts with a pair of electrodes separated with a relative large gap in an electrolyte (Figure 3). When applying a bias voltage between the two electrodes, metal atoms are etched off from the anode and deposited onto the cathode. The etching takes place all over the anode surface, but the deposition is localized to a protruding point on the cathode, which is the closest point to the anode. Since this protruding point sees more ions etched off the anode, it grows faster towards the anode than the rest of the cathode. This reinforces the initial advantage and makes it grow even faster. Consequently, the gap narrows and disappears eventually when a point contact is formed between the two electrodes.

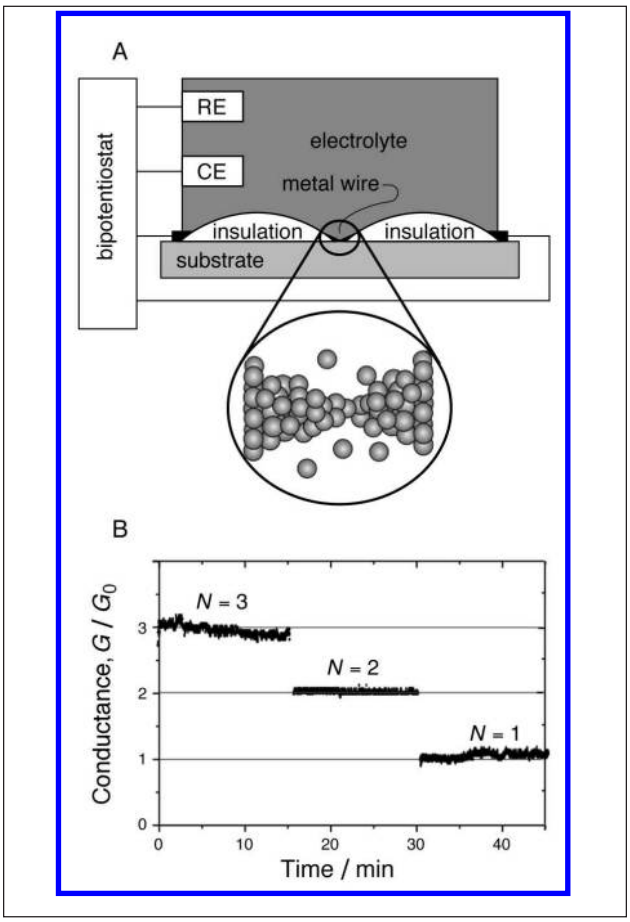

Figure 2. (A) Electrochemical fabrication of atomic-scale metal wires. A metal wire is attached to a insulating substrate. The wire is coated with wax except for a small section that is exposed to electrolyte for etching. The electrochemical potential of the wire is controlled by a bipotentiostat with a reference electrode (RE) and a counter electrode (CE).

(B) Electrochemically fabricated atomic-scale Cu wires with conductance at N = 1, 2, and 3 quantum steps.

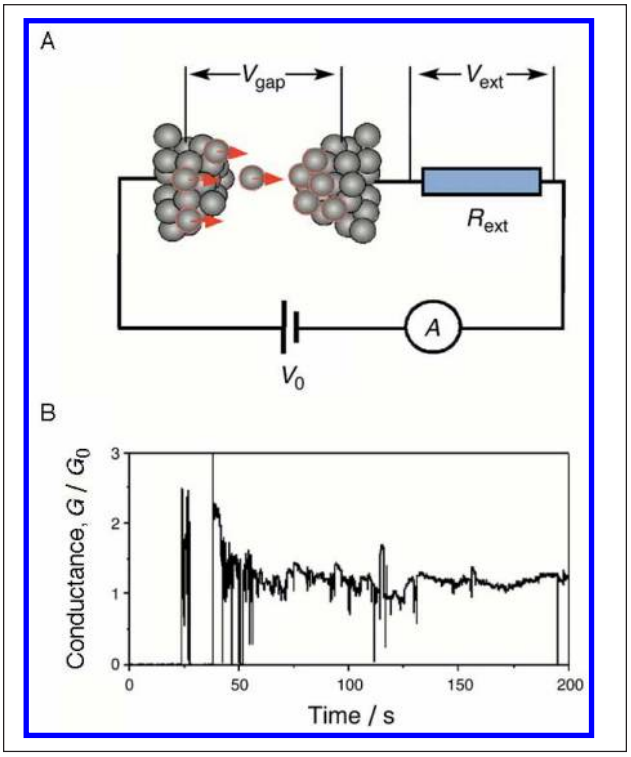

Figure 3. Fabrication of metal nanowires with a self-limiting electrochemical method:

(A) Metal atoms etched off left electrode are deposited onto the right electrode by applying a voltage between the electrodes with an external resistor (R_{ext}) in series. As the gap between the two electrodes shrinks, the gap resistance decreases, which results in a drop in etching and deposition voltage and eventually terminates the etching/deposition processes.

(B) Choosing a R_{ext} < 12.9 kΩ, a wire with quantized conductance can be fabricated. The conductance change during the formation of a contact (R_{ext} = 3 kΩ and V_0 = 1.2 V). The large conductance fluctuations corresponding to constant breakdown and reformation of the contact are due to electromigration.

To control the formation of the contact between the electrodes, the etching and deposition processes must be terminated immediately after a desired contact is formed, which is achieved by connecting one electrode in series with an external resistor (R_{ext}). The effective voltage for etching and deposition is given by

$$V_{gap} = \frac{R_{gap}}{R_{gap} + R_{ext}} V_0 \qquad (13)$$

where R_{gap} is the resistance between the two electrodes, and V_0 is the total applied bias voltage. Initially, the gap is large, so R_{gap} is very large because it is solely determined by ionic conduction (leakage current) between the electrodes, which is minimized by coating the electrodes with insulation layers. In this case, $V_{gap} \sim V_0$ according to eq 13, so the etching and deposition take place at maximum speed and the gap quickly narrows. When the gap reduces to a few nm or less, R_{gap} begins to decrease because of electron tunneling across the gap and the electrochemical processes stop. Eventually, a contact with quantized conductance is formed between the two electrodes.

The conductance (normalized against G_0) between two Cu electrodes during electrochemical etching and deposition in water with R_{ext} preset at 3 kΩ (< 12.9 kΩ) is shown in Figure 3. The initial conductance due to ionic conduction is negligibly small in comparison to G_0. A few minutes after applying a 1.2 V voltage, the conductance suddenly jumps to ~2 G_0 and the deposition terminates as a contact is formed between the electrodes. However, the initial contact breaks within seconds probably because the structure is in a metastable state and the conductance drops back to zero. Once the contact is broken, the voltage across the electrodes goes back to the maximum value, according to eq 13, and the etching and deposition start over again. Indeed, several seconds later, a new contact with conductance near 1 G_0 is reformed. So, the method has a self-repairing mechanism.

Applications

Most research efforts so far have been directed to a better understanding of electrochemical fabrication metallic quantum wires. However, a number of applications based on the phenomenon have been proposed and explored.

Motivated by the possibility of chemical sensing applications, molecular and ionic adsorption onto atomic-scale metal wires have been studied. Xu et al. have observed the changes in the conductance of gold quantum wires upon adsorption of F^-, Cl^-, Br^-, and I^- *(49)*. The quantity of conductance change correlates well with the adsorption strengths of the anions (Figure 4). Because the wire is typically a few atoms long, enough to accommodate only a few ions, the sensitive dependence of the conductance on the adsorption suggests a method to detect a single or a few ions. It has also been observed that the conductance of metallic quantum wires decreases upon molecular adsorption *(50, 51)*. The largest conductance drop occurs for the wires with conductance at the lowest quantum step, and the drop diminishes quickly at higher steps as the quantum ballistic regime is replaced by the classical regime. Similar to anions, the conductance change correlates with the binding strength of the molecules to the metal wires. One possible mechanism of the adsorbate-induced conductance change is the scattering of the conduction electrons in the quantum wires by the adsorbate.

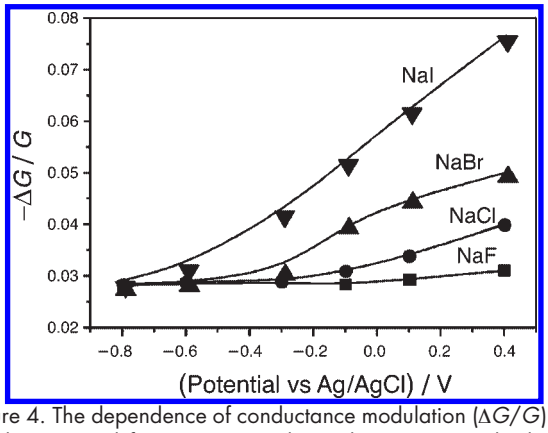

Figure 4. The dependence of conductance modulation ($\Delta G/G$) versus the potential for Au wires with conductance near the lowest quantum step (G = 1 G_0) in the electrolytes containing F^-, Cl^-, Br^-, and I^- anions. The adsorption increases with the potential, and the adsorption strengths of anions are in the order of $F^- < Cl^- < Br^- < I^-$.

Penner et al. have demonstrated sensitive detection of a number of gas molecules using various metal nanowires fabricated using graphite step edges as templates *(44, 52)*.

Another effort toward chemical sensor applications is the detection of metal ions. The experiment starts wi™- a pair of electrodes separated with a nanometer scale gap. By adjusting the electrodes at an appropriate potential, metal ions in the electrolyte can be deposited into the gap and form a quantum wire that is detected as quantized increase in the conductance. Using this method, metal ions (e.g., Cu^{2+} and Pb^{2+}) at concentration less than l nM have been detected *(53)*. The specificity of the method relies on the fact that different metals can be deposited or etched at different potentials, which resembles the anodic stripping technique.

Another area of applications using metallic quantum wires is magnetic materials and devices. One of the important magnetic phenomena is the magnetoresistance effect, which describes the dependence of the resistance of a material on an applied magnetic field. This effect allows one to read (measure) magnetic field by simply measuring the resistance of a material, and the technique has been used in today's computer hard disks. The magnetoresistance effect is usually weak and prohibits us from measuring a weak magnetic field, so it is highly desired to find a material that exhibits a large magnetoresistance effect. Garcia et al. reported a magnetoresistance effect as large as 400–700% in Ni point contacts fabricated by electrodeposition *(54–55)*. More recently, Chopra and Hua observed a remarkable magnetoresistance effect greater than 3000% in Ni point contact at room temperature and in a weak magnetic field (a few hundred oersteds) *(56)*. These findings are anticipated to lead to applications in magnetic storage devices and spintronics.

Summary

Electrochemical methods have been widely used to fabricate various nanostructures because of their simplicity and flexibility. The main focus of this article is on the fabrication of metallic quantum wires. These wires are as thin as a single atom and as short as a few nm. Because they are naturally connected to two macroscopic electrodes, the conductance of the system (wires and electrodes) can be readily measured,

which allows one to constantly monitor the conductance during fabrication and use conductance quantization as a signature to guide the fabrication. This technique is different from other methods that rely on using a template or local STM or AFM probe to control the dimensions and shape of the fabricated nanostructures. Electrochemical methods are clearly limited to conductive materials, but a number of complementary fabrication techniques have been developed to fabricate insulating and semiconducting nanowires.

Acknowledgments

The author thanks K. W. Hipps, H. S. White, and J. Hoh for valuable comments; C. Z. Li, S. Boussaad, H. X. He, and B. Xu for their contributions; and NSF and DOE for financial support.

Literature Cited

1. Landauer, R. *IBM J. Res. Dev.* **1957,** *1,* 223.
2. Ferry, D. K.; Goodnick, S. M. *Transport in Nanostructures;* Cambridge University Press: Cambridge, 1997.
3. Bogachek, E. N.; Scherbakov, A. G.; Landman, U. *Phys. Rev. B* **1997,** *56,* 1065.
4. Kittle, C. *Introduction to Solid State Physics,* 3rd ed.; John Wiley & Sons: New York, 1967
5. van Wees, B. J.; van Houten, H.; Beenakker, C. W. J.; Williams, J. G.; Kouwenhowen, L. P.; van der Marel, D.; Foxon, C. T. *Phys. Rev. Lett.* **1988,** *60,* 848.
6. Wharam, D. A.; Thornton, T. J.; Newbury, R.; Pepper, M.; Ahmed, H.; Frost, J. E. F.; Hasko, D. G.; Peacock, D. C.; Ritchie, D. A.; Jones, G. A. C. *J. Phys. C* **1988,** *21,* 209.
7. Gimzewski, J. K.; Moller, R. *Phys. Rev. B* **1987,** *36,* 1284.
8. Pascual, J. I.; Mendez, J.; Gomez-Herrero, J.; Baro, A. M.; Garcia, N.; Binh, V. T. *Phys. Rev. Lett.* **1993,** *71,* 1852.
9. Olesen, L.; Lægsgaard, E.; Stensgaad, I.; Besenbacher, F.; Schiotz, J.; Stoltze, P.; Jacobsen, K. W.; Norskov, J. K. *Phys. Rev. Lett.* **1994,** *72,* 2251.
10. Costa-Kramer, J. L.; Garcia, N.; Garcia-Mochales, P.; Serena, P. A. *Surf. Sci.* **1995,** *342,* L1144.
11. Landman, U.; Luedtke, W. D.; Salisbury, B. E.; Whetten, R. L. *Phys. Rev. Lett.* **1996,** *77,* 1362.
12. Ohnishi, H.; Kondo, Y.; Takayanagi, K. *Nature* **1998,** *395,* 780.
13. Li, C. Z.; Tao, N. J. *Appl. Phys. Lett.* **1998,** *72,* 894.
14. Li, C. Z.; Bogozi, A.; Huang, W.; Tao, N. J. *Nanotechnology* **1999,** *10,* 221.
15. Snow, E. S.; Park, D.; Campbell, P. M. *Appl. Phys. Lett.* **1996,** *69,* 269.
16. Morpurgo, A. F.; Marcus, C. M.; Robinson, D. B. *Appl. Phys. Lett.* **1999,** *14,* 2082.
17. Bard, A. J.; Faulkner, L. R. *Electrochemical Methods;* John Wiley and Sons, Inc.: New York, 1980.
18. Nyffenegger, R. M.; Penner, R. M. *Chem. Rev.* **1997,** *97,* 1195.
19. Tao, N. J.; Li, C. Z.; He, H. X. *J. Electroanal. Chem.* **2000,** *492,* 81.
20. Li, W. J.; Nirtanen, J. A.; Penner, R. M. *Appl. Phys. Lett.* **1992,** *60,* 1181.
21. Li, W.; Hsiao, G. S.; Harris, D.; Nyffenegger, R.; Virtanen, J. A.; Penner, R. M. *J. Phys. Chem.* **1996,** *100,* 20103.
22. Potzschke, R. T.; Staikov, G.; Lorenz, W. J.; Wiesbeck, W. *J. Electroanal. Chem.* **1999,** *146,* 141.
23. Hofmann, D.; Schindler, W.; Kirchner, J. *Appl. Phys. Lett.* **1998,** *73,* 3279.
24. Nagahara, L. A.; Thundat, T.; Lindsay, S. M. *Appl. Phys. Lett.* **1990,** *57,* 270.
25. Ross, C. B.; Sun, L.; Crooks, R. M. *Langmuir* **1993,** *9,* 632.
26. Xie, Z.-X.; Kolb, D. M. *J. Electroanal. Chem.* **2000,** *481,* 177.
27. Xie, Z. X.; Cai, X. W.; Tang, J.; Chen, Y. A.; Mao, B. W. *Chem. Phys. Lett.* **2000,** *322,* 219.
28. Schuster, R.; Kirchner, V.; Xia, X. H.; Bittner, A. M.; Ertl, G. *Phys. Rev. Lett.* **1998,** *80,* 5599.
29. Matsumoto, K.; Ishii, M.; Segawa, K.; Oka, Y.; Vartanian, B. J.; Harris, J. S. *Appl. Phys. Lett.* **1996,** *68,* 34.
30. Nyffenegger, R. M.; Penner, R. M. *J. Phys. Chem.* **1996,** *100,* 17041.
31. Kolb, D. M.; Ullmann, R.; Will, T. *Science* **1997,** *275,* 1097.
32. Kolb, D. M. *Electrochem. Acta* **2000,** *45,* 2387.
33. Possin, G. E. *Rev. Sci. Instrum.* **1970,** *41,* 772.
34. Williams, W. D.; Giordano, N. *Rev. Sci. Instrum.* **1984,** *55,* 410.
35. Cheng, I. F.; Whiteley, L. D.; Martin, C. R. *Anal. Chem.* **1989,** *61,* 762.
36. Menon, V. P.; Martin, C. R. *Anal. Chem.* **1995,** *67,* 1920.
37. Thurn-Albrecht, T.; Steiner, R.; DeRouchey, J.; Stafford, C. M.; Huang, E.; Bal, M.; Tuominen, M.; Hawker, C. J.; Russell, T. P. *Adv. Mater.* **2000,** *12,* 787.
38. Hong, B. H.; Bae, S. C.; Lee, C.-W.; Jeong, S.; Kim, K. S. *Science* **2001,** *294,* 348.
39. Coffer, J. L.; Bigham, S. R.; Li, X.; Pinizzotto, R. F.; Rho, Y. G.; Pirtle, R. M.; Pirtle, I. L. *Appl. Phys. Lett.* **1996,** *69,* 3851.
40. Braun, E.; Eichen, Y.; Sivan, U.; Ben-Yoseph, G. *Nature* **1998,** *391,* 775.
41. Zhang, Y.; Dai, H. J. *Appl. Phys. Lett.* **2000,** *77,* 3015.
42. Zach, M. P.; Ng, K. H.; Penner, R. M. *Science* **2000,** *290,* 2120.
43. Zach, M. P.; Inazu, K.; Ng, K. H.; Hemminger, J. C.; Penner, R. M. *Chem. Mat.* **2002,** *14,* 3206.
44. Favier, F.; Erich, C. W.; Zach, M. P.; Benter, T.; Penner, R. M. *Science* **2001,** *293,* 2227.
45. Nakabayashi, S.; Sakaguchi, H.; Baba, R.; Fukushima, E. *Nano Lett.* **2001,** *2,* 507.
46. Li, J. Z.; Yamada, Y.; Murakoshi, K.; Nakato, Y. *Chem. Commun.* **2001,** *21,* 2170.
47. Li, J. Z.; Kanzaki, T.; Murakoshi, K.; Nakato, Y. *Appl. Phys. Lett.* **2002,** *81,* 123.
48. Boussaad, S.; Tao, N. J. *Appl. Phys. Lett.* **2002,** *80,* 2398.
49. Xu, B. Q.; He, H. X.; Tao, N. J. *J. Am. Chem. Soc.* **2002,** *124,* 13568.
50. Li, C. Z.; He, H. X.; Bogozi, A.; Bunch, J. S.; Tao, N. J. *Appl. Phys. Lett.* **2000,** *76,* 1333.
51. Bogozi, A.; Lam, O.; He, H. X.; Li, C. Z.; Tao, N. J.; Nagahara, L. A.; Amlani, I.; Tsui, R. *J. Am. Chem. Soc.* **2001,** *123,* 4585.
52. Murray, B. J.; Walter, E. C.; Penner, R. M. *Nano Lett.* **2004,** *4,* 419.
53. Rajagopalan, V.; Boussaad, S.; Tao, N. J. *Nano Lett.* **2003,** *3,* 851.
54. Garcia, N.; Munoz, M.; Qian, G.; Rohrer, H.; Saveliev, I.; Zhao, Y. *Appl. Phy. Lett.* **2001,** *79,* 4550.
55. Garcia, N.; Qiang, G. G.; Saveliev, I. G. *Appl. Phys. Lett.* **2002,** *80,* 1785.
56. Chopra, H. D.; Hua, S. Z. *Phys. Rev. B.* **2002,** *66,* 020403.

Editor's Note

An experiment in which nanowires are synthesized appears on pp 765–768 in this issue.